

#### Megaron

https://megaron.yildiz.edu.tr - https://megaronjournal.com DOI: https://doi.org/10.14744/megaron.2025.03266



## **Article**

# Material analyses and field applications for the conservation of archeological remains found in the aerial cable car station construction site in Hatay (Türkiye)

Dilek EKŞİ AKBULUT<sup>1\*</sup>, Mehmet UĞURYOL<sup>2</sup>, Burak HAZNEDAR<sup>3</sup>

<sup>1</sup>Department of Architecture, Yıldız Technical University, Istanbul, Türkiye <sup>2</sup>Department of Conservation and Restoration of Cultural Property, Yıldız Technical University, Istanbul, Türkiye <sup>3</sup>Teb Mimarlik, Istanbul, Türkiye

#### **ARTICLE INFO**

Article history
Received: 05 July 2024
Revised: 03 July 2025
Accepted: 09 September 2025

#### Key words:

Antioch; archaeological conservation; consolidation by injection grout; earthquake; material analysis.

#### **ABSTRACT**

During the constructions carried out within the scope of the Aerial Cable Car Project planned by Hatay Metropolitan Municipality, archaeological remains were discovered in İplik Pazarı District where a station was going to be built, and upon that discovery, rescue excavation works were started in 2012 for the conservation of the remains. This article deliberates the material analyses of the archeological remains performed during the preparation of the survey, restitution, and restoration projects; the field inspections and the small-scale intervention trials on the remains carried out during the implementation phase of the cable car project; the suggestions developed for the conservation of the remains based on these studies, and the conservation practices carried out in line with these suggestions. In this context, the determined characteristics of the stone, brick, and mortar samples taken from the remains were given, recommendations for the consolidation mortar and injection grout compositions were presented, and the field applications carried out in line with these recommendations were outlined. Other conservation activities were also addressed, such as the methods used in the fight against algae formation on the wall surfaces and works conducted for repairing terracotta pipes and sarcophagi.

Cite this article as: Akbulut, D. E., Uguryol, M., & Haznedar, B. (2025). Material analyses and field applications for the conservation of archeological remains found in the aerial cable car station construction site in Hatay (Türkiye). Megaron, 20(3):346–360.

#### INTRODUCTION

Being a region that has a moderate climate and fertile lands located at the crossroads that connect Anatolia to Syria and Palestine via the Çukurova Plain and that harbors the most expedient ports to reach the Mediterranean from Mesopotamia, Hatay has been one of the most sought-after

destinations susceptible to flows of immigration and has been the host land for many cultures throughout history. Antakya, the central town of Hatay, is one of the settlements most destroyed by earthquakes throughout history. Antakya experienced its first known earthquake in 148 BC (Adams & Barazangi, 1984). Earthquakes encountered in

<sup>\*</sup>E-mail adres: dileksi@yahoo.com



<sup>\*</sup>Corresponding author

130 BC, 37, 115, 458, 525, and 526 AD are recognized as the major earthquakes that hit the city. The most severe of these, and the one that caused the most loss of life, was the earthquake that occurred in 526. In this earthquake, 250-300,000 people died (Beyen et al., 2003). The city is known to be subject to essential earthquakes in 528, 551, 557, 560, 577, 588, 750, 841, 859, 868, 1053, 1090, 1157, 1169, 1303, 1406, 1759, 1787, 1822, and 1872 (Beyen et al., 2003). Earthquakes in 1157 and 1169 caused extensive damage to Bakras Castle. Two other severe earthquakes that occurred in the area in 1615 and 1872 caused great destruction in Antakya and its villages (T.C. Hatay Valiliği, 2019). Later on, the earthquakes that happened in Hatay were light and therefore non-damaging (Beyen et al., 2003). Unfortunately, after the earthquake on February 6, 2023, great destruction and loss of life were experienced in the center of Hatay and the surrounding districts, and many cultural assets were demolished or damaged.

The route of the Aerial Cable Car Project, planned by Hatay Metropolitan Municipality, is adjacent to the Phyrminus (Hamşen) River, which has been partially covered and taken under the road passing over it today. Upon discovering archaeological remains during the works carried out in the project area (İplik Pazarı District), a rescue excavation was started promptly in 2012. The findings obtained during the rescue excavation indicate that this area is a part of the settlement belonging to the city of Antiokheia, and the architectural structures and finds unearthed in the area point out the presence of Roman, Byzantine, Islamic, and Ottoman Periods, respectively.

article discusses the conservation aforementioned archeological remains completed before the earthquake on February 6, 2023. In this context, results of the laboratory examinations carried out on the samples taken from the walls, procedures and practices for the consolidation of the walls by pointing and grout injection according to the outcomes of the laboratory work and field inspections, the removal of algae, the cleaning and assembly of earthenware pipe and terracotta sarcophagus fragments, and furthermore, a preliminary observation about the general condition of the consolidated walls after being subjected to the earthquake, are presented. The laboratory work revealed the types of the sampled stones and the mechanical properties of the sampled stones, bricks, and mortars. The ingredients of the consolidation mortars (pointing mortars) were determined according to the binder-aggregate ratio and granulometry of the mortar samples identified by laboratory analyses. Consolidation of the walls included grout injection since the field inspections showed the presence of internal gaps in the walls that needed to be filled to overcome discontinuities and achieve structural integrity. The composition of the grout was decided through simple tests applied to trial grouts at the worksite. Through finalizing the last part of the fieldwork, including the removal of algae with biocide application and the cleaning and repair of earthenware pipes and terracotta sarcophagi, in-situ conservation and presentation of the architectural remains with related archaeological finds were performed within the frame of a holistic approach.

## THE WORKSITE: ARCHAEOLOGICAL REMAINS AND STATION CONSTRUCTION

During the archaeological work, rooms of a settlement belonging to the Roman Period were discovered (Figure 1), whereas remains from the Byzantine and Ottoman periods were also unearthed, which are all well below the elevation level currently in use due to the stratification built up over the centuries. Through the archaeological work, it was determined that modifications, including the use of spolia, and repairs were made during each main period of the building (Pamir & Sezgin, 2016). Although the remains carry features from different periods, the structure is assumed to be a Villa Urbana type Roman building in general terms. The entrance of the building, which has commercial units facing the street on both sides, appears to be located in the north direction, adjacent to the atrium (main hall). The entrance section, where the triclinium (dining room) and atrium are placed and covered with mosaics, can also be read as an example of a quintessential garden arrangement, which is frequently seen in Roman villas. The dining area, which is adjacent to this garden at the entrance, is believed to be located at the center of the building, with other spatial usages surrounding these two main areas.

A monochrome (white) figureless floor mosaic is laid in the entrance of the villa, and the Three-Panel Mosaic with Figures (Figure 2) located in the dining hall is dated to the 3<sup>rd</sup> or 4<sup>th</sup> century AD. The Greek inscription on the mosaic conveys enjoying, having fun, and cheering up (Pamir & Sezgin, 2016).



**Figure 1**. General view of the excavation area.



Figure 2. Three-Panel Mosaic with figures.

While the Aerial Cable Car Project construction was ongoing, a transparent protective platform was built over the excavation area, using mainly steel and glass, to protect the remains from external factors and allow them to be seen by visitors. The aerial cable car sub-station structure that will rise over the remains is located approximately 8 m above the glass platform. The superstructure of the aerial cable car is associated with the remains by means of its main load-bearing elements. At the locations of the load-bearing elements, the archaeological remains were temporarily removed and partially moved back after the construction was completed. For the main load-bearing elements, foundations were dug by hand. The glass platform is designed to enable the remains to be perceived holistically, as well as to combine the different elevations currently in use around the excavation area and establish the relationship of the navigation route with them.

# DETERMINATION OF THE PROPERTIES OF THE BUILDING MATERIALS

#### On-site inspections and sampling

During the on-site inspections conducted in November 2014, the ground floor floors of the building were determined to be made of limestone slabs, whereas the walls were built with stone and brick (Figure 3; Figure 4). Two types of stones and three types of bricks of different heights (thickness) were determined throughout the building. The heights of the bricks are 40 mm, 35 mm, and 50 mm; the width and length of a 35 mm-high brick, of which all dimensions can be measured, were observed to be approximately 300x300 mm in size, whereas the mortar in the joints was seen to vary between 20 and 40 mm in height. In addition, on some bricks, 8 mm wide and 1 mm deep diagonal grooves were identified that were opened to increase the adherence between brick and mortar (Figure 4).

In order to determine the other properties of the building materials and to be able to make material

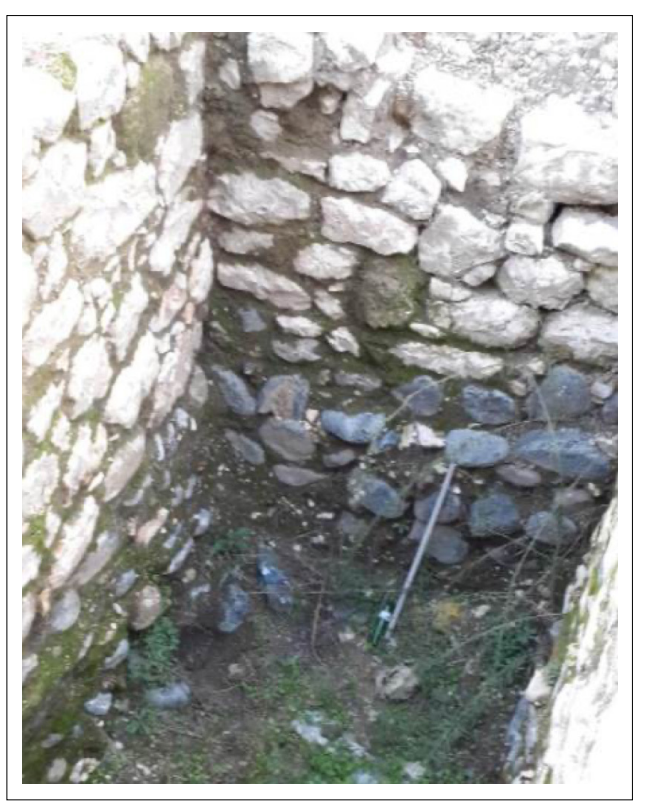


**Figure 3**. The different types of stones that were used throughout the structure.



**Figure 4**. The grooves on a brick.

recommendations that would be appropriate to be used for the consolidation works, six stone, three brick, and three mortar samples were taken from the locations identified in the Roman building remains. Locations of the samples were marked on the scaled survey drawings (Figure 5). Building materials that were loosened or disintegrated in their original location were determined through a visual inspection and were chosen for sampling to minimize the probable damage to the adjacent sound materials in better condition.

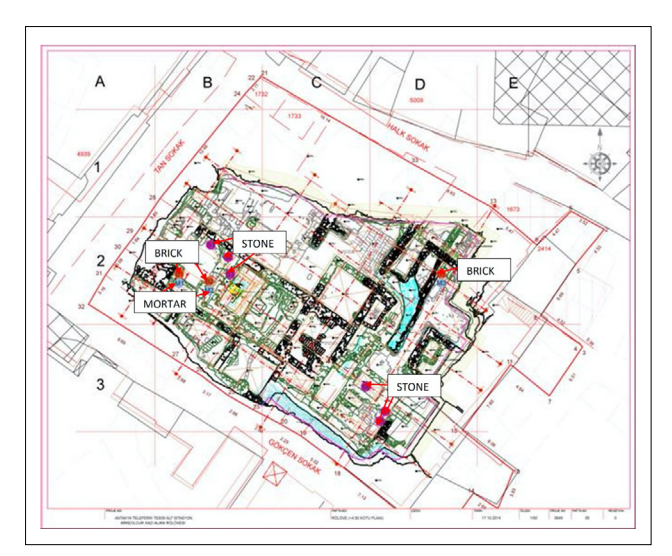


**Figure 5.** Location of the samples (purple marks represent natural stones, orange marks represent bricks and blue marks represent mortars).

#### Laboratory works and findings

The samples taken from the site were brought to the Construction Materials Laboratory of the Faculty of Civil Engineering at Yıldız Technical University. 43 specimens (24 stone, 13 brick, and 6 mortar) were prepared from the samples. The results of the examinations, analyses, and tests carried out on these samples and specimens are given below

Natural Stones: Through visually conducted on-site and laboratory inspections, two types of natural stones were identified as being used in the structure: sedimentary and igneous rocks. The sedimentary rocks used throughout the building are two types of limestone. One of them is a massive, non-porous, fine-grained, crack-free, non-clay-bearing, strong, limestone (represented by samples Stone 1 and Stone 3) with a light white-cream color, and has a weathering degree of W1 according to the ISRM (International Society for Rock Mechanics) classification (Chala & Rao, 2021; Brown, 1981). The other one is a yellowish-cream colored, strong, nonclay-bearing dolomitic limestone (represented by sample Stone 2), which contains few dissolution voids, and has a weathering degree of W2. Samples taken from another rock type, which was seen to be used less frequently in the structure, revealed to be igneous plutonic rocks. The samples examined in this group were lead gray-colored, strong, microlithic gabbro-type fine-grained basic rocks (represented by samples Stone 4 and Stone 6) with weathering degrees of W1-W2, and a slightly serpentinized gabbro-type basic rock (represented by sample Stone 5) with a weathering degree of W2-W3.

The natural stone samples brought to the laboratory were cut with a stone-cutting machine; thus, cube samples of (50±5) mm were prepared in accordance with TS EN 1926 (TSE, 2013). The uniaxial compression test was carried out with a 60-ton capacity loading device. The uniaxial compressive strength (N/mm²) was calculated as the ratio of the breaking load to the cross-section of the specimen (Table 1).

Within the scope of physical properties of the stone samples, real density, apparent density, and total and open porosity of the specimens were determined (Table 2) according to TS EN 1936 (TSE, 2007). Moreover, their water absorption (Table 2) was identified, and capillary water absorption curves were drawn (Figure 6) to calculate the capillary water absorption coefficient in line with TS EN 15801 (TSE, 2010) using cube specimens prepared with dimensions of 50±5 mm. However, since there was very little to no capillary water absorption on the surfaces of the specimens within the first hour, the regression line could not be drawn on the graph, and the capillary water absorption coefficient could not be determined.

Limestones used throughout the building were detected to be extremely high-strength, and the samples taken from them have an average uniaxial compressive strength of 103.6 N/mm² according to TS EN 1926 (TSE, 2013). Results of the uniaxial compression test applied to the limestone specimens are presented in Table 1. The physical tests applied to the limestones (Table 2) revealed an average apparent

Table 1. Uniaxial compressive strength of the stone specimens.

Sample code	Uniaxial compressive strength (N/mm²)	Average uniaxial compressive strength (N/mm²)
Stone 1	139.4	115.7±17.0
	107.0	
	100.6	
Stone 2	124.6	106.3±12.9
	96.9	
	97.4	
Stone 3	119.7	88.7±23.0
	81.4	
	64.9	
Stone 4	84.9	104.7±24.5
	139.3	
	89.9	
Stone 5	98.1	*
Stone 6	84.2	123.3±30.2
	127.6	
	158.0	

<sup>\*</sup> Due to the dimensions and geometry of the stone sample, only one specimen could be prepared in accordance with the standard.

Sample code	Apparent density, Pb (g/cm³)	Real density, P <sub>r</sub> (g/cm <sup>3</sup> )	Total porosity, p (%)	Water absorption	
				By weight (%)	By volume (%)
Stone 1	2.7	2.9	7.6	0.5	1.3
Stone 2	2.7	3.0	8.7	0.7	1.8
Stone 3	2.7	2.7	1.9	0.2	0.5
Stone 4	3.0	3.1	4.8	0.1	0.4
Stone 5	2.6*	2.8	8.8	2.5*	6.5*
Stone 6	3.0	3.1	1.8	0.1	0.3

**Table 2.** Results of the physical tests applied to the stone specimens.

<sup>\*</sup> Due to the dimensions of the stone sample. only one specimen could be prepared in accordance with the standard. The relevant results should be disregarded as they pertain to this single specimen. which also exhibited cracks.

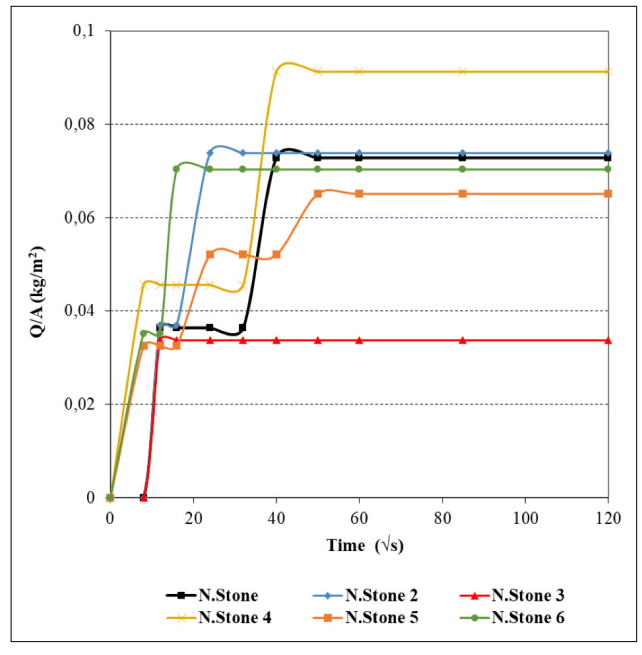


**Figure 6**. Average capillary water absorption curves of the stone specimens.

density, real density, open porosity, and total porosity of 2.7 g/cm<sup>3</sup>, 2.9 g/cm<sup>3</sup>, 1.2%, and 6.1%, respectively. The average water absorption by weight of these limestone samples is nearly 0.5%.

Samples taken from the lead gray-colored, extremely high-strength (average uniaxial compressive strength 108.7 N/mm²) magmatic gabbro rocks found at the lower parts of the walls have an average apparent density of 3.0 g/cm³, a real density of 3.1 g/cm³, an average open porosity of 0.4%, a total porosity of 3.3% according to TS EN 1936 (TSE, 2007), and an average water absorption by weight value of 0.1%. Capillary water absorption of the specimens from both gabbro groups was negligible. Results of the physical tests and uniaxial compression test applied to the gabbro specimens are presented in Tables 1 and 2.

Bricks: Three prismatic specimens were prepared for testing from each of the three brick samples, resulting in a total of nine specimens. The uniaxial compressive strength of the specimens was determined and converted to normalized compressive strength (Table 3) according to TS EN 772-1 (TSE, 2012a). Normalized compressive strength values of the specimens prepared from the three brick samples of three different heights (40 mm/B-1, 35 mm/B-2, and 50 mm/B-3) used in the building are 10.5, 14.5, and 4.3 N/mm² on average, respectively, and meet the minimum average compressive strength requirement (5.0 N/mm²) for medium-strength clay bricks specified in TS EN 771-1 (TSE, 2011).

Physical properties of the brick samples (Table 4) were determined through tests for real density, apparent density, and total and open porosity of the specimens according to TS EN 1936 (TSE, 2007), along with a water absorption test (Table 4). Brick specimens' capillary water absorption coefficients (Table 5) were determined in line with TS EN 15801 (TSE, 2010), using three prismatic specimens prepared from each sample, resulting in a total of nine specimens.

Brick specimens were detected to have an average apparent density of 1.8 g/cm³, a real density of 2.8 g/cm³, a total porosity of 35%, an open porosity of 29% according to TS EN 1936 (TSE, 2007) a water absorption ratio by weight of 17%, an average capillary water absorption coefficient of 0.1684 kg/(m²·√sec) according to TS EN 15801 (TSE, 2010) and it ranged from 0.0643 to 0.3680 kg/(m²·√sec). The capillary water absorption curves given in Figure 7 were utilized to determine the capillary water absorption coefficient.

**Mortars:** Of the mortar samples brought to the laboratory, prismatic specimens could only be obtained from sample no. 3. Prepared samples were subjected to a uniaxial compression test. The compressive strengths (N/mm²) of the specimens are shown in Table 6.

**Table 3.** Uniaxial compressive strength of the brick sprecimens.

Sample code	Uniaxial compressive strength (N/mm²)		Normalized uniaxial compressive strength (N/mm²)	
	Value for each specimen	Average value	Value for each specimen	Average value
Brick 1				
height (thickness): 40 mm	19.1	16.9±1.7	11.9	10.5±1.1
	16.4		10.1	
	15.1		9.4	
Brick 2				
height (thickness): 35 mm	21.5	23.9±1.7	13.3	14.5±0.8
	25.2		15.0	
	25.2		15.2	
Brick 3				
height (thickness): 50 mm	8.3	6.7±1.3	5.3	4.3±0.8
	6.5		4.2	
	5.2		3.3	

**Table 4.** Results of the physical tests applied to the brick specimens.

Sample code	Apparent density, Pb (g/cm³)	Real density, Pr (g/cm³)	Total porosity, p (%)	Water absorption	
				By weight (%)	By volume (%)
Brick 1	1.8	2.8	35.9	16	29
Brick 2	1.8	2.7	31.5	16	28
Brick 3	1.7	2.8	38.5	18	31

**Table 5.** Capillary water absorption coefficients of the brick specimens.

Sample code	Capillary water absorption coefficient (kg/(m²·√sn))	Average capillary water absorption coefficient (kg/(m²·√sn))
Brick 1	0.0628	0.0643
	0.0729	
	0.0572	
Brick 2	0.0749	0.0730
	0.0769	
	0.0672	
Brick 3	0.3705	0.3680
	0.3869	
	0.3467	

The point load strength index (Is (50)) in TS 699 (TSE, 2009) was determined by the point load test applied to the mortar samples with suitable geometry and dimensions. According to the literature, the ratio between the point

 Table 6. Uniaxial compressive strength of the mortar specimens.

Sample code	Uniaxial compressive strength (N/mm²)	Average uniaxial compressive strength (N/mm²)
Mortar 3	0.9	1.2±0.5
	1.9	
	0.9	

load strength index and uniaxial compressive strength (strength conversion factor) of historical mortars varies between 6 and 10 (Polat Pekmezci, 2012; Polat Pekmezci & Ersen, 2010; Gürdal et al., 2011). In a study on lime mortars, the relationship between uniaxial compressive strength and point load strength index was investigated and the strength conversion factor was determined as 8 (Ulukaya et al., 2012). Using this value, the point load test results were converted to uniaxial compressive strength, and the results are given in Table 7. Tests for the determination of physical properties could only be applied to prismatic samples obtained from sample 3. The results of these tests are given in Table 8.

**Table 7.** Point load test results of the mortar specimens.

Sample code	Corrected point load strength index, $I_{s(50)}(N/mm^2)$	Converted uniaxial compressive strength (N/mm²)	Average converted uniaxial compressive strength (N/mm²)
Mortar 1	0.20	1.6	1.7±0.1
	0.23	1.9	
Mortar 2	0.34	2.7	2.0±0.8
	0.29	2.3	
	0.12	0.9	
Mortar 3	0.07	0.5	$0.9 \pm 0.7$
	0.23	1.8	
	0.04	0.3	

Table 8. Results of physical tests applied to the mortar specimens.

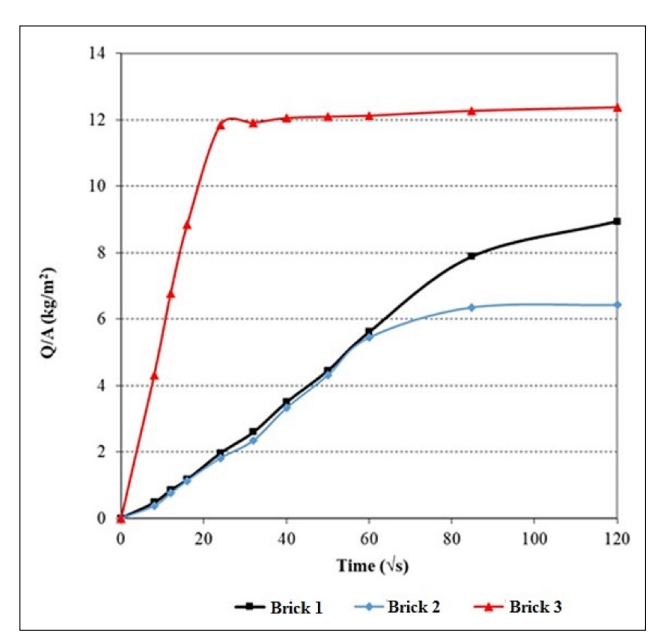
Sample code	Apparent density, Pb (g/cm³)	Real density, Pr (g/cm³)	Total porosity, p (%)	Water absorption	
				By weight (%)	By volume (%)
Mortar 3	1.7	2.6	33.6	19	32

Table 9. Capillary water absorption coefficients of mortars.

Sample code	Capillary water absorption coefficient (kg/(m²·√sec))	Average capillary water absorption coefficient (kg/(m²·√sec))
Mortar 3	0.3799	0.3359
	0.3319	
	0.2960	

The capillary water absorption coefficients of the mortar samples were determined according to TS EN 15801 (TSE, 2010). Three specimens could be prepared only from mortar sample no. 3 based on the dimensions and geometrical qualities specified in the standard. The capillary water absorption coefficients of those three prismatic samples are presented in Table 9. The capillary water absorption curve given in Figure 8 is used to determine the capillary water absorption coefficient.

Acid loss analysis was performed to roughly estimate the binder:siliceous aggregate ratio of the mortar samples taken from different locations (Figure 5). Specimens weighing at least 50 g were taken from the mortar samples, pulverized, treated with 10% hydrochloric acid, and mixed for 60 minutes, and the weight loss ratio of each after acid treatment was determined by filtering them through filter paper. According to the results given in Table 10, the binder:aggregate ratio varies between 1:2 and 1:4. The aggregates retained after acid treatment were subjected to sieve analysis to determine their grain size distributions, as presented with the granulometry curves in Figure



**Figure 7**. Average capillary water absorption curves of the brick specimens.

9. Accordingly, the maximum aggregate grain size was determined to be 8 mm for all mortar samples.

Weight losses of the mortars against temperature changes were investigated by loss on ignition analysis to determine the ignition loss at 200-600°C which represents the output of structurally bound water (H<sub>2</sub>O), and the ignition loss above 600°C which represents the release of carbon dioxide (CO<sub>2</sub>) as a result of the calcination of carbonated lime, since the hydraulic properties of the mortars are

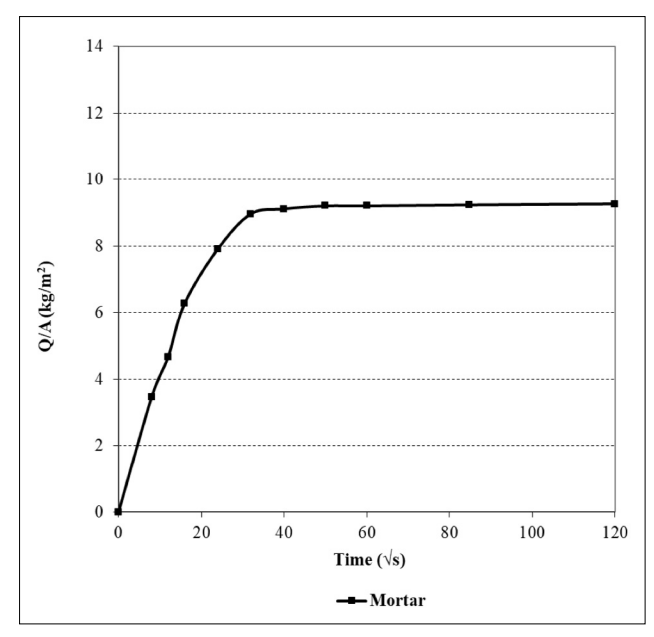


**Figure 8**. Average capillary water absorption curve of the mortar specimens.

**Table 10.** Acid loss percentages and roughly determined binder-aggregate ratios of the mortar specimens.

Sample no.	Acid Loss (%)	Binder:Aggregate
Mortar 1	20.3	1:4
	20.0	1:4
Mortar 2	39.1	1:2
	33.5	1:2
Mortar 3	23.4	1:3
	25.3	1:3

evaluated according to the ratio of lost carbon dioxide and water percentages ( $CO_2/H_2O$ ). If this ratio is less than 10, it is accepted that the mortars show hydraulic properties, and if it is between 10 and 35, it is assumed that they do not show hydraulic properties (Moropoulou et al., 1995a; Moropoulou et al., 1995b; Bakolas et al., 1995; Bakolas et al., 1998; Moropoulou et al., 2000). Accordingly, the ratio of lost carbon dioxide and water percentages ( $CO_2/H_2O$ ) of the examined specimens being less than 10 indicates that the sampled mortars have hydraulic properties (Table 11).

#### Recommendation for consolidation mortar

The laboratory examinations indicated that the three sampled mortars were lime mortars showing hydraulic properties with a maximum aggregate grain size of 8 mm and having lime:aggregate ratios (calculated roughly through the acid loss analysis) between 1:2 and 1:4 (the average corresponds to 1:3). Taking into account these characteristics, an average mortar mixing ratio that is

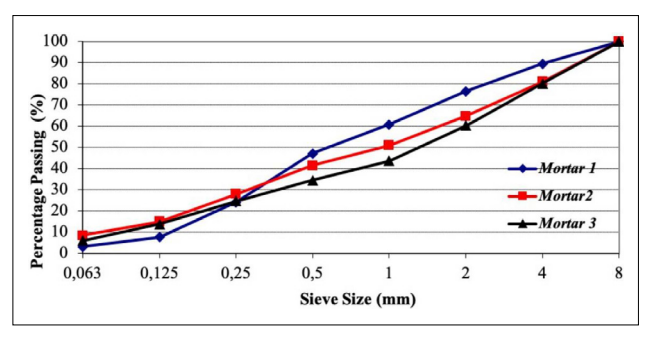


Figure 9. Grain size distribution of the aggregates.

Table 11. Ignition loss results in mortar specimens.

Sample no.	Loss on Ignition		CO <sub>2</sub> /H <sub>2</sub> O
	200-600°C	<600°C	
Mortar 1	2.4	5.4	2.2
	2.8	5.9	2.1
Mortar 2	3.0	17.0	5.6
	3.3	18.9	5.7
Mortar 3	2.7	13.8	5.1
	3.0	15.7	5.3

considered suitable for use in the consolidation of the structure is given in Table 12. In the mixture, silicabased aggregate with a maximum grain size of 8 mm and natural hydraulic lime in NHL 3.5 class in accordance with TS EN 459-1 (TSE, 2012b) or alternatively lime putty (air lime) with pozzolan as the binder, are recommended to be used, and the grain distribution of the aggregates is suggested to be in accordance with the granulometry curve in Figure 10.

### **FIELDWORK**

Conservation interventions were started in 2018 on the basis of the findings obtained as a result of the examinations and determinations made on the wall remains in the archaeological area and the material analyses carried out in the laboratory.

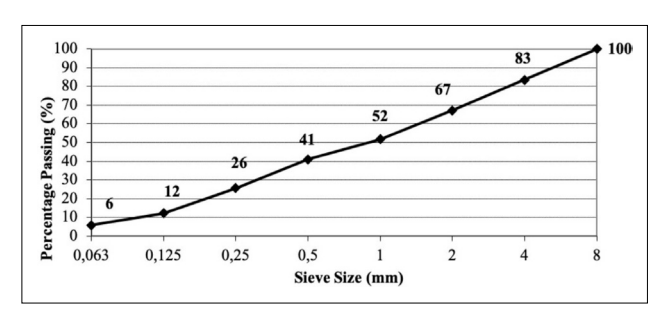


**Figure 10**. Suggested granulometry values for aggregate to be used in consolidation mortar.

#### Consolidation of the walls

Condition of the walls: In September 2018, partial wall removal work started in the regions where the well foundations correspond. The removed wall stones were numbered and properly kept in a storage area (Figure 11). A scaffold was erected for the work related to well foundations. The wells were dug by hand.

Although the walls were being supported with sandbags against rain, it was predicted that precipitation would pose a threat in winter conditions, especially to the weak masses containing soil, rubble, and broken terracotta fragments (Figure 12) present between some stone walls at different elevations.

#### Preparation and application of consolidation mortars:

For the consolidation of the walls in the excavation area, a mortar mixture was proposed based on the material analyses report, and the materials to be used in this mixture were requested to be supplied from the contractor company. A sample from the tuff stone fragments, which were supplied by the contractor company from Nevşehir region and recommended for use in the mortar mix as a pozzolan, was taken to the Construction Materials Laboratory of the Faculty of Civil Engineering at Yıldız Technical University to perform pozzolanic activity tests.

XRD analysis was performed using a GNR brand APD 2000-PRO model device, and the minerals contained in the powdered tuff specimen (d<63  $\mu$ m) were determined qualitatively. According to the XRD analysis, quartz, plagioclase (anorthite), calcite, augite, and hematite minerals were observed in the diffraction patterns of the examined material (Figure 13). No distinct amorphous phase could be detected due to the XRD analysis of the examined sample. In order to determine the chemical composition of the material under investigation, XRF (X-Ray Fluorescence Spectrometry) analysis was performed on powder samples (d<63  $\mu$ m) prepared in the laboratory using a Bruker brand S8 Tiger model device. The results

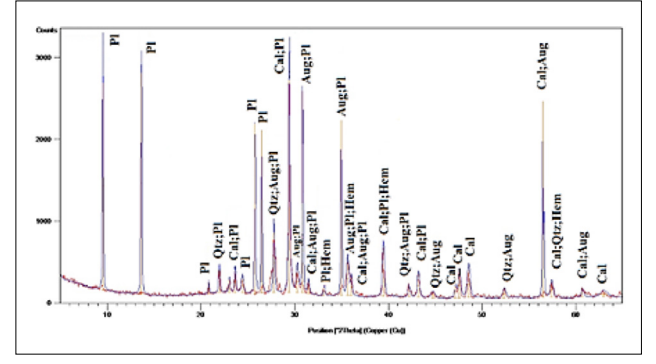


Figure 11. Numbered wall stones.

are given in Table 13 as the elemental components of the sample, in terms of oxides and their percentage by weight. Accordingly, the sample examined contains mainly silicon and calcium and, secondarily, aluminum, magnesium, and iron elements. The total of "SiO<sub>2</sub> + Al<sub>2</sub>O<sub>3</sub> + Fe<sub>2</sub>O<sub>3</sub>" by weight included in the material is 48.80%. This value does



**Figure 12.** Weak masses containing soil, rubble, and broken terracotta fragments that are prone to erosion by rain.



**Figure 13**. XRD diffraction patterns of the examined sample (Aug: Augite; Cal: Calcite; Hem: Hematite; Pl: Plagioclase; Qtz: Quartz).

not meet the minimum limit value of 70%, which is one of the conditions specified in TS 25 (TSE, 2008) and required for the material to be qualified as natural pozzolan.

Within the scope of the test conducted according to TS 25, the compressive strength of three mortar specimens prepared in 4x4x16 cm molds with a mixture of air lime, sand, and the tuff sample to be tested was determined. Due to the TS 25 standard, if the compressive strength of the lime mortars prepared with the material tested is 4 MPa and above, the tested material is accepted as pozzolan. Since the compressive strengths of the tuff specimens are below 4 MPa, the tuff sample in question is not accepted as pozzolan according to TS 25.

When the results of the mineralogical analysis (XRD), chemical analysis (XRF), and strength tests are taken into account, the examined material cannot be qualified as a natural pozzolan for cement and concrete as specified in TS 25. However, according to the results of the Frattini test, which is based on the chemical titration method and performed in accordance with TS EN 196-5 (TSE, 2012c), it was determined that the material in question showed low pozzolanic activity. In addition, blast furnace slag and fly ash, which are widely used artificial pozzolans, were also analyzed in order to compare the pozzolanic activity of the material under investigation. The results showed that the pozzolanic activity of the examined tuff fragments was lower than that of blast furnace slag and fly ash (Figure 14). In order to increase the pozzolanic effect, and thus the lime mortar strength, the contractor was advised to reduce the grain size below 63 or 75 microns by grinding the tuff fragments.

During the site visit in December 2018, a consolidation mortar that complies with the granulometry determined by the analyses was prepared with the materials requested from the contractor, such as sieves, lime, aggregates, and tuff fragments ground into powder. This mixture, which is applied to a small section of a wall, contains air lime (lime putty) as the binder, river sand as the aggregate, and tuff stone (recommended by the contractor) powder as the pozzolan, and acrylic dispersion (Primal AC33 equivalent) as an admixture. As in the original mortar, the mortar was prepared to gain hydraulic properties by using pozzolan and air lime. However, it was seen that the mortar applied did not provide sufficient pre-hardening and strength after a week. In order to increase the strength, two different trial mortars with hybrid binders were prepared by mixing natural hydraulic lime (NHL 3.5) which was indicated in the material analyses report, with air lime in certain

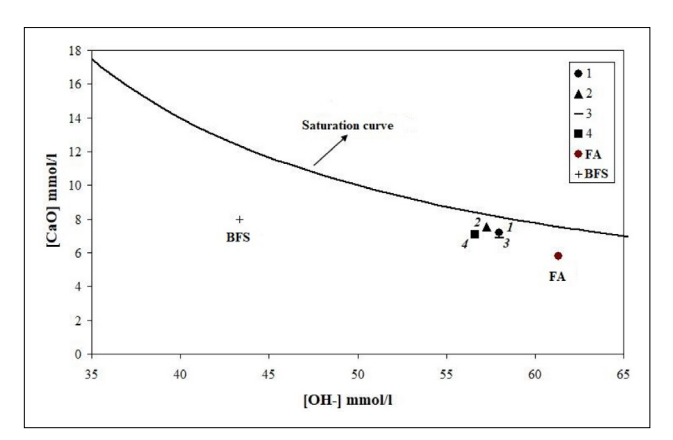


**Figure 14**. Frattini test results of four specimens from the same tuff sample (1, 2, 3, and 4), along with a blast furnace slag (BFS) specimen and a fly ash (FA) specimen. The plots of the four tuff specimens are situated near the saturation curve, indicating that they exhibit low pozzolanic activity.

proportions. These mortars, which also contain river sand, tuff fragments, and tuff dust, were applied next to the previously applied mortar (Figure 15).

Mortars containing only NHL as the binder were also prepared, but it was observed that the workability of the mortars with the hybrid binder was better than that of the mortars containing only NHL as the binder. Two weeks after the application, it was realized that the strength of the mortars with hybrid binders, whose workability was also high, was at a satisfactory level. Therefore, a mortar with a hybrid binder composed of lime putty and NHL in equal proportions was decided to be used.

The weak masses containing soil, rubble, and broken terracotta fragments shown in Figure 16 that are prone to getting damaged by precipitation were reinforced by coating them with a hydraulic lime mortar of higher strength than the one designated for pointing the walls (Figure 15). NHL 5 type natural hydraulic lime and river sand were used for this purpose, in line with the proportions given in Table 12.

**Injection application:** Inspections carried out on the site gave rise to the thought that an injection application was also necessary for the consolidation of the walls. Thereupon, simple tests were carried out to determine the ingredients of an efficient injection grout. For this purpose, first of all, various blends intended for injection with different water, aggregate, binder, and admixture proportions were mixed at the worksite. Then tests were carried out with these grouts prepared using NHL, limestone powder (under 100 microns)

**Table 12.** The ratios of the components of the recommended consolidation mortar by weight.

Lime	Aggregate	Water
1	3	The amount of water should be determined in accordance with the flow values indicated in TS EN 1015-2 (TSE 2000a), and by preliminary tests to be carried out in accordance with TS EN 1015-3 (TSE 2000b).

**Table 13.** Chemical composition of the tuff sample in terms of oxides.

Constituent	Wt %
SiO <sub>2</sub>	30.10
$Al_2O_3$	9.44
$Fe_2O_3$	9.26
MgO	6.73
CaO	25.06
Na <sub>2</sub> O	1.68
$K_2O$	1.18
${ m TiO}_2$	1.21
$P_2O_5$	0.29
SO <sub>3</sub>	0.21
BaO	0.04
CuO	0.11
NiO	0.02
MnO	0.15
SrO	0.06
$Cr_2O_3$	0.04
ZnO	0.07
$\mathrm{ZrO}_{2}$	0.03
Cl	0.05
F	0.20
Ignition loss (1050°C/3 hours)	14.02

and tuff powder (under 75 microns). The grout mixtures were poured into 60-mL injectors standing vertically and also into small cups. It was observed at the end of one week that samples containing equal amounts of tuff powder and



**Figure 15.** Previously applied lime mortar with a lighter color and fresh trial mortars with the hybrid binder (they can be distinguished by the color differences between them) applied to a small section infested by algae.

limestone powder took a longer time to set, shrank, and bled more compared to those containing only limestone powder as the aggregate (Figure 17). These results suggested that tuff powder did not sufficiently react with air lime, which is a non-hydraulic component of NHL, and did not contribute enough to the setting process. Hence, the results were considered compatible with the results of the pozzolanic activity tests applied. With respect to this, the tuff powder was decided not to be used in the next trial blends prepared at the worksite. In this context, trial blends containing NHL, limestone powder, water, and acrylic dispersion (Primal AC33 equivalent) were prepared. To be able to ensure sufficient fluidity by using the minimum amount of water, the amount of water in each blend prepared was reduced compared to the amount used



Figure 16. A weak mass consolidated by covering it with a lime mortar containing NHL 5.



**Figure 17**. Injectors and cups used to monitor the bleeding water, shrinkage amount, and setting status of the trial grouts prepared at the worksite for injection.

**Table 14.** Grout composition in parts by volume.

Natural Hydraulic	Limestone	Water	Acrylic
Lime	Powder		Dispersion
1	1	1.25	0.1

in the previous one. The composition shown in Table 14 was chosen as the most suitable grout mixture for consolidation and applied to the walls, starting from the bottom parts (Figure 18).

## Removal of Algae

As a cleaning proposal against algae formation on the walls (Figure 15; Figure 18; Figure 19) was required, it was suggested that algae removal should start after the consolidation of the walls was completed and the rainy weather passed away, and initially mechanical cleaning was advised to be done with plastic brushes and water. Following this step, brushing with a benzalkonium chloride containing biocide such as Preventol RI 80 or Preventol RI 50, which are commonly used for biologically infested archaeological and historic masonry materials (Macchia et al., 2022; Antonelli et al., 2024; Berti et al., 2024), and then rinsing with water was recommended. This procedure was applied first to a small area, and its effectiveness was monitored for a certain period. Since success was achieved, it was then applied to the zones infested by algae.

# Conservation of Earthenware Pipe and Terracotta Sarcophagus

The excavated earthenware pipe and terracotta sarcophagus fragments (Figure 20) were cleaned and assembled in the workshop set up on the worksite to be displayed in situ. The fragments were assembled in sandboxes using epoxy resin (Figure 21). To remove loose deposits, water and plastic brushes were used, while concretions were removed using scalpels and dental instruments.



**Figure 18**. Grout application through injection on a wall infested with algae.



**Figure 19.** Algae formation on the horizontal surfaces of the walls.

#### CONCLUSION

Following the rescue excavation, mortar, brick, and stone samples were obtained to determine the properties of the construction materials that constitute the architectural remains to be conserved. On-site inspections and laboratory examinations showed that two different types of natural stones were used throughout the building, namely limestones, including dolomitic limestone, and igneous rocks, including microlithic gabbro-type basic rocks, that



**Figure 20**. Earthenware pipes (on the left) and a terracotta sarcophagus (on the right) broken into pieces.



**Figure 21**. Earthenware pipe fragments that were cleaned and assembled in the workshop set up at the worksite.

were in good condition in terms of preservation. Laboratory work also indicated that the bricks were sound since they meet the minimum strength requirements for medium strength clay bricks. However, the joints of the stones and bricks and the core of the walls became widely empty due to the deterioration of the original mortars. Therefore, the first step of the conservation work was decided to be the consolidation of the walls since the work coincided with the winter season, and since precipitation has become the leading factor that threatens the wall remains by weakening



Figure 22. General view of the site after the earthquake.

the remaining mortars. Supports created with sandbags temporarily protected the walls before the consolidation was performed.

A lime mortar for consolidation was prepared in accordance with the results obtained from the laboratory work applied to the original mortar samples. Based on the material analyses, trials were made on the site to optimize the mortar blend suitable for consolidation in terms of color, texture, workability, and strength. Since the pozzolanic activity tests performed on the tuff obtained from Nevşehir region revealed that this material showed low pozzolanic activity, it was concluded that using this material together with air lime would not be enough to achieve the desired success. The trials carried out on the site with tuff-bearing mortars also supported this view. For that reason, it was deemed appropriate to use the tuff together with natural hydraulic lime and, to increase its pozzolanic effect, to use it after it was ground very finely. In this context, pulverized tuff was used as a color component rather than as a natural pozzolan. The mortar applied consisted of natural hydraulic lime (NHL 3.5), air lime, blended in accordance with the binder:aggregate ratio specified in the material analyses report, river sand with a small amount of tuff dust compatible with the granulometry specified in the same report, and acrylic admixture.

The results obtained from the inspections carried out on the site gave rise to the thought that an injection application was also required for the consolidation of the walls. In this regard, an injection grout was designed by preparing various blends with different water, aggregate, binder, and admixture proportions and subjected to simple tests at the worksite. In this context, injectors and cups were used to monitor the bleeding water, shrinkage amount, and setting status of the trial mortar blends containing NHL, limestone powder, water, and acrylic dispersion (Primal AC33 equivalent) for injection. The grout mixture considered most suitable for consolidation was applied to the walls, starting from the bottom parts.

Furthermore, prognosticating that precipitation would pose a threat to the weak masses containing soil, rubble, and broken terracotta fragments present at different elevations, these masses were reinforced by coating them with a hydraulic lime mortar of higher strength than the one designated for pointing the stone walls.

Interventions to control the biological activity were also carried out as part of the conservation of the walls. In this respect, a biocide containing benzalkonium chloride succeeded in the removal and prevention of the algae, though dampness should be controlled under the glass platform and cleaning operations should be repeated if infestation occurs again. Moreover, assembly and cleaning works performed on the earthenware pipes and terracotta sarcophagus fragments were carried out successfully under the conditions available at the worksite.

It should finally be noted that, after the earthquake, the site is not allowed to be visited or inspected yet; however, according to the view from outside the archaeological site, the consolidated remains seem sound and undamaged by the earthquake (Figure 22).

**ACKNOWLEDGEMENT:** The authors would like to acknowledge Prof. Dr. Mustafa YILDIRIM, Prof. Dr. Nabi YÜZER, Assit. Prof. Dr. Didem OKTAY and Assit. Prof. Dr. Serhan ULUKAYA for performing the laboratory work.

**ETHICS:** There are no ethical issues with the publication of this manuscript.

**PEER-REVIEW:** Externally peer-reviewed.

**CONFLICT OF INTEREST:** The authors declared no potential conflicts of interest with respect to the research, authorship, and/or publication of this article.

**FINANCIAL DISCLOSURE:** The authors declared that this study has received no financial support.

#### **REFERENCES**

- Adams, R. D., & Barazangi, M. (1984). Seismotectonics and seismology in the Arab region: A brief summary and future plans. *Bulletin of the Seismological Society of America*, 74(3), 1011–30. https://doi.org/10.1785/BSSA0740031011
- Antonelli, F., Iovine, S., Perasso, C. S., Macro, N., Gioventù, E., Capasso, F. E., & Bartolini, M. (2024). Essential oils and essential oil-based products compared to chemical biocides against microbial patinas on stone cultural heritage. *Coatings*, *14*(12), 1546. https://doi.org/10.3390/coatings14121546
- Bakolas, A., Biscontin, G., Contardi, V., Franceschi, E., Moropoulou, A., Palazzi, D., & Zendri, E. (1995). Thermoanalytical research on traditional mortars

- in Venice. *Thermochimica Acta*, 269–70, 817–28. https://doi.org/10.1016/0040-6031(95)02574-X
- Bakolas, A., Biscontin, G., Moropoulou, A., & Zendria, E. (1998). Characterization of structural Byzantine mortars by thermogravimetric analysis. *Thermochimica Acta*, 321(1–2), 151–60. https://doi. org/10.1016/S0040-6031(98)00454-7
- Berti, L., Arfelli, F., Villa, F., Cappitelli, F., Gulotta, D., Ciacci, L., Bernardi, E., Vassura, I., Passarini, F., Napoli, S., & Goidanich, S. (2024). LCA as a complementary tool for the evaluation of biocolonization management: The case of Palazzo Rocca Costaguta. *Heritage*, 7(12), 6871–90. https://doi.org/10.3390/heritage7120318
- Beyen, K., Erdik, M., Mazmanoğlu, C., & Ekmekçioğlu, Z. (2003). The seismic activity of Antakya from past to present and the evaluation of what needs to be done in the light of an international conference [Antakya'nın geçmişten günümüze sismik aktivitesi ve yapılması gerekenlerin bir uluslararası konferansın ışığında değerlendirilmesi]. *Turkish Engineering News [Turk Muhendislik Haberleri]*, 423, 51–3. https://eski.imo.org.tr/resimler/dosya\_ekler/2342e-1b8ee9d659\_ek.pdf?dergi=172
- Brown, E. T. (1981). Rock characterization, testing and monitoring: ISRM suggested methods. Pergamon Press.
- Chala, E. T., & Rao, K. S. (2021). Evaluation of weathered rock mass strength and deformation using weathering indices. *IOP Conference Series Earth and Environmental Science*, 833, 012194. https://doi.org/10.1088/1755-1315/833/1/012194
- Gürdal, E., Altaş, K. G., & Özgünler, S. A. (2011). Investigation of the characteristics of the horasan mortars used in the early Byzantine period religious structures located in Istanbul [İstanbul'da bulunan Erken Bizans dönemi dini yapılarında kullanılan horasan harçların özelliklerinin incelenmesi]. Foundation Restoration Annual [Vakıf Restorasyon Yıllığı], 2, 63–72.
- Macchia, A., Strangis, R., De Angelis, S., Cersosimo, M.,
  Docci, A., Ricca, M., Gabriele, B., Mancuso, R., & La
  Russa, M. F. (2022). Deep eutectic solvents (DESs):
  Preliminary results for their use such as biocides in the building cultural heritage. *Materials*, 15(11), 4005. https://doi.org/10.3390/ma15114005
- Moropoulou, A., Bakolas, A., Michailidis, P., Chronopoulos, M., & Spanos, Ch. (1995b). Traditional technologies in Crete providing mortars with effective mechanical properties. *Transactions on The Built Environment*, 15, 151–61.
- Moropoulou, A., Bakolas, A., & Bisbikou, K. (1995a). Characterization of ancient, Byzantine and later historic mortars by thermal and X-ray diffraction techniques. *Thermochimica Acta*, 269–70, 779–95.

- https://doi.org/10.1016/0040-6031(95)02571-5
- Moropoulou, A., Bakolas, A., & Bisbikou, K. (2000). Investigation of the technology of historic mortars. *Journal of Cultural Heritage*, 1(1), 45–58. https://doi.org/10.1016/S1296-2074(99)00118-1
- Moropoulou, A., Bakolas, A., Moundoulas, P., & Cakmak, A. S. (1999). Compatible restoration mortars for Hagia Sophia earthquake protection. *Transactions on the Built Environment*, 41, 521–31.
- Pamir, H., & Sezgin, N. (2016). The sundial and convivium scene on the mosaic from the rescue excavation in a late antique house of Antioch. *Adalya*, 19, 247–80. https://dergipark.org.tr/en/pub/adalya/issue/54568/743807
- Pekmezci, P. I. (2012). Characterization of mortars used in some historical structures in the Çukurova region (Cilicia) and recommendations for repair mortars [Çukurova bölgesindeki (Kilikya) bazı tarihi yapılarda kullanılan harçların karakterizasyonu ve onarım harçları için öneriler] [PhD dissertation]. Istanbul Technical University.
- Pekmezci, P. I., & Ersen, A. (2010). Characterization of Roman mortars and plasters in Tarsus (Cilicia–Turkey). In J. Válek, C. Groot, & J. J. Hughes (Eds.), 2nd Conference on Historic Mortars HMC2010 and RILEM TC 203-RHM Final Workshop (pp. 317–24). RILEM Publications SARL.
- T.C. Hatay Valiliği. (2019). *The city of all times: Hatay [Tüm zamanların şehri: Hatay]*. Retrieved Sep 10, 2025, from http://www.hatay.gov.tr/hatay-tarihine-genel-bakis
- TSE (Turkish Standards Institution). (2000a). Methods of test for mortar for masonry Part 2: Bulk sampling of mortars and preparation of test mortars. TS EN 1015-2.
- TSE (Turkish Standards Institution). (2000b). Methods of test for mortar for masonry Part 3: Determination of consistence of fresh mortar (by flow table). TS EN

- 1015-3.
- TSE (Turkish Standards Institution). (2007). Natural stone test methods Determination of real density and apparent density and of total and open porosity. TS EN 1936.
- TSE (Turkish Standards Institution). (2008). Natural pozzolan (trass) for use in cement and concrete – Definitions, requirements and conformity criteria. TS 25.
- TSE (Turkish Standards Institution). (2009). Natural building stones Methods of inspection and laboratory testing. TS 699.
- TSE (Turkish Standards Institution). (2010). Conservation of cultural property Test methods Determination of water absorption by capillarity. TS EN 15801.
- TSE (Turkish Standards Institution). (2011). Specification for masonry units Part 1: Clay masonry units. TS EN 771-1.
- TSE (Turkish Standards Institution). (2012a). Methods of test for masonry units Part 1: Determination of compressive strength. TS EN 772-1.
- TSE (Turkish Standards Institution). (2012b). Building lime Part 1: Definitions, specifications and conformity criteria. TS EN 459-1.
- TSE (Turkish Standards Institution). (2012c). Methods of testing cement Part 5: Pozzolanicity test for pozzolanic cement. TS EN 196-5.
- TSE (Turkish Standards Institution). (2013). *Natural stone* test methods Determination of uniaxial compressive strength. TS EN 1926.
- Ulukaya, S., Yüzer, N., Selçuk, M. E., & Yıldırım, M. (2012). Investigation of the experimental methods applied in the definition of historical lime mortars [Tarihi kireç harçlarının tanımlanmasında uygulanan deney yöntemlerinin irdelenmesi]. 100 Years in Civil Engineering Technical Congress [İnşaat Mühendisliğinde 100 Yıl Teknik Kongresi], Türkiye, 22 17 November 2012, vol.1, pp.171–180.